Predictive velocity control in a hilly terrain over a long look-ahead horizon

Ahad Hamednia, Nikolce Murgovski, Jonas Fredriksson

Department of Electrical Engineering, Chalmers University of Technology, 41296 Gothenburg, Sweden (e-mail: hamednia@chalmers.se).

Abstract: This paper presents a computationally efficient velocity control of vehicles driving in a possibly hilly terrain and over long look-ahead horizons that may stretch to hundreds of kilometers. The controller decouples gear scheduling into an offline optimization problem, from the remaining optimization problem that governs two real-valued states. One of the states, the travel time, is adjoined to the objective by applying the necessary optimality conditions, which results into an online optimization problem that has kinetic energy as the single state. Finally an inner approximation is proposed for the online problem to obtain a quadratic program that can be solved efficiently. The efficiency of the proposed controller is shown for different horizon lengths.

Keywords: Predictive control, Cruise control, Offline gear scheduling, Sequential quadratic programming

1. INTRODUCTION

The depletion of oil reserves, global warming and pollutant emissions are recently being considered as alarming issues in automotive industry due to economic, environmental and health reasons. One promising way that mitigates the consequences from the excessive usage of oil is to improve the vehicular energy efficiency, thus reducing oil consumption and simultaneously reducing harmful emissions.

Vehicle's energy efficiency can be improved by intelligent usage of its energy storage units, which in the case of a conventional vehicle include the kinetic, potential and chemical (fuel) storage. To this end, velocity profile of the vehicle can be controlled over a narrow speed interval, where proper gear is selected. For instance, the vehicle's speed can decrease when climbing uphill and gradually increase while rolling downhill, which results in less energy dissipation at the braking pads. This type of driving belongs to a category, which is so-called economic driving. For long-haulage trucks, the energy consumption and CO2 emissions can be reduced up to 10 % by economic driving (Barkenbus, 2010).

Rule-based control strategies are suitable for implementation of the behaviour of speed varying within the interval, where topographic profiles are relatively simple. On the other hand, model-based control strategies are suggested for more complex topographic profiles, where various optimal control algorithms are employed to coordinate the energy use. The model-based control strategies can be mainly classified into dynamic programming (DP)-based, non DP-based and mixed methods.

DP (Bellman, 1957) is the most commonly used optimization method in the technical literature for finding global optimum of nonlinear, non-convex and mixed-integer problems. A DP-based method is proposed by Hellström et al. (2009, 2010), to optimize velocity trajectory, where trip time is constrained and close-to-optimal fuel consumption is achieved. A two-layer planning approach is presented by Heppeler et al. (2016), where energy management system (EMS) and economic driving are considered together to have optimized gear shifting, velocity trajectories and torque split of a hybrid electric vehicle. However, exponential increase of computational time with increasing the number of state variables and control signals, i.e. the so-called *curse of dimensionality*, is the main drawback of using DP.

In order to alleviate the amount of computational effort, several approaches have been proposed that adjoin system dynamics to the objective function (Hellström et al., 2010; Lindgärde et al., 2015; van Keulen et al., 2010, 2011). A numerical approach, based on Pontryagin's Minimum Principle (PMP) (Pontryagin et al., 1962) is employed by van Keulen et al. (2014) for power split control problem in hybrid electric vehicles. Although PMP methods are computational-efficient for control over long distance intervals, they do not provide the same computational advantage for optimal control problems where states often activate their bounds, especially the methods that relay on a single shooting for solving a two-point boundary value problem (van Keulen et al., 2010, 2011). Another faster approach, which characterizes simultaneous component sizing and energy management of plug-in hybrid electric vehicles (PHEV)s into convex optimization framework is proposed by Murgovski et al. (2012); Pourabdollah et al. (2013). By using this approach it is possible to handle the large-size problems with very long driving cycles. However, the main drawback is that the approach cannot be applied to mixed-integer problems, which arise when, e.g., gear scheduling ought to be optimized.

Another portion of the conducted research benefits from combination of DP and other methods. Such approaches have been proposed by Johannesson et al. (2015a,b); Murgovski et al. (2016); Hovgard et al. (2018), where real-valued decisions, e.g., planing optimal velocity, are made by convex optimization, while integer decisions are made by DP. These approaches have also been shown to be promising when considering surrounding traffic (Johannesson et al., 2015b), or cooperative energy management of multiple vehicles (Murgovski et al., 2016; Hovgard et al., 2018). Other proposed approaches rely on a combination of DP and PMP (Ngo et al., 2012; Uebel et al., 2017). To investigate the impact of optimized gear shifting on fuel economy the combined DP-PMP method is presented by Ngo et al. (2012), where gear and engine on/off are regarded as integer states. Online-capable EMS using the DP-PMP method is reported by Uebel et al. (2017).

The previously mentioned online implementable methods are suitable for predictive control over moderately long look-ahead horizons, in the range of 5-20 km. The goal of this paper is to develop an online implementable predictive controller over longer look-ahead horizons that may stretch to the end of the route, i.e to hundreds of kilometers. The purpose of the controller is to provide a target set for low-level controllers with a limited look-ahead horizon, such as those discussed previously. In the case of conventional vehicles, the typical target set includes the maximum travel time, while in the case of a PHEV, the target set may also include the allowed change in battery energy.

In particular, this paper considers optimization of velocity and gear trajectory of a heavy duty vehicle, on horizons that possibly stretch over 100 km. Several steps are proposed to decrease computational effort, while preserving sufficient amount of modeling details that capture the general trend of predictive state trajectories that derive from longitudinal vehicle dynamics. These steps include 1) a problem decomposition into two sub-problems, which include an online optimization of velocity and travel-time trajectory and an offline optimization of gear shifting strategy, 2) a combination of an indirect PMP solution and a direct nonlinear programming for reducing the number of states in the online optimization sub problem, and 3) a real-time iteration (RTI) sequential quadratic programming (SQP), which allows a single quadratic program (QP) to be solved in a moving horizon framework. Although the intended usage of the proposed method is in a model predictive control (MPC) framework (Mayne et al., 2000), this paper focuses on the derivation of the QP formulation for a single MPC stage.

The outline of current paper is as follows. The paper starts with powertrain modelling in Section 2. The optimization control problem is formulated in Section 3. Bi-level computational efficient algorithm is presented in Section 4. Simulation results are given in Section 5 and finally the paper is concluded in Section 6.

2. POWERTRAIN MODELLING

This section introduces the powertrain model of a conventional vehicle, which includes a transmission and an internal combustion engine (ICE).

2.1 Longitudinal vehicle dynamics

The conventional vehicle is modeled as a lumped mass, where traveled distance, s, and vehicle speed, v, are state variables

$$\dot{s}(t) = v(t) \tag{1}$$

$$m\,\dot{v}(t) = F_{\mathrm{w}}(t) + F_{\mathrm{brk}}(t) - F_{\alpha}(s) - F_{\mathrm{air}}(v) \tag{2}$$

with m denoting the total vehicle mass, and F_{w} and F_{brk} the non-negative force delivered by ICE at the wheel side of the vehicle and the non-positive braking force, respectively. In (2), traveled distance and vehicle speed are functions of t, however it is omitted from $F_{\alpha}(s)$ and $F_{\mathrm{air}}(v)$ for simplicity. The nominal aerodynamic drag and forces that depend on road gradient α are modeled as

$$F_{\alpha}(s) = mg\left(\sin(\alpha(s)) + c_r\cos(\alpha(s))\right) \tag{3}$$

$$F_{\mathrm{air}}(v) = \frac{\rho_a c_d A_f v^2(t)}{2} \tag{4}$$

where g is the gravitational acceleration, c_r is rolling resistance coefficient, ρ_a is air density, c_d is aero-dynamic drag coefficient and A_f is vehicle frontal area. The vehicle dynamics (2) are nonlinear due to the trigonometric function of traveled distance (3) and the quadratic term in the aerodynamic drag (4).

2.2 Change of independent variable

To overcome the nonlinearity in (3) a change of independent variable is proposed, where decisions are planed with respect to travel distance, s, instead of travel time. This introduces the travel time, $t(s)$, as a state in the problem. In addition, the nonlinearity in (4) is removed by a change of state variable, where kinetic energy

$$E(s) = \frac{mv^2(s)}{2} \tag{5}$$

is used instead of velocity. These transformations are non-approximate as long as the studied vehicle does not stop or change direction of its movement. Similar variable changes have been applied previously for optimal control of vehicles (Murgovski et al., 2013a; Lipp and Boyd, 2014; Johannesson et al., 2015b; Murgovski et al., 2015, 2016; de Castro et al., 2016). Consequently, the new governing equations of the studied system are

$$t'(s) = \sqrt{\frac{m}{2E(s)}} \tag{6}$$

$$E'(s) = F_{\mathrm{w}}(s) + F_{\mathrm{brk}}(s) - \tilde{c_{\mathrm{a}}}E(s) - F_{\alpha}(s) \tag{7}$$

where t' is used as a short hand notation for $\mathrm{d}t/\mathrm{d}s$, $E'(s) = mv(s)v'(s)$ and the coefficient in (7) is calculated as $\tilde{c_a} = \rho_a c_d A_f/m$. It can be noticed that (7) becomes a linear equation, although (6) is still nonlinear. A method for dealing with the nonlinearity in (6) is presented later, in Section 4.

2.3 Engine model

For given engine speed values, ω, engine torque, M, and fuel mass rate, $\mu(\omega, M)$, steady-state data of a diesel engine is gathered using a detailed model presented by Wahlström and Eriksson (2012). Fig. (1) shows the obtained fuel mass rate represented as brake specific fuel consumption (BSFC), together with the maximum delivered torque $M_{\max}(\omega)$, which is a function of engine speed.

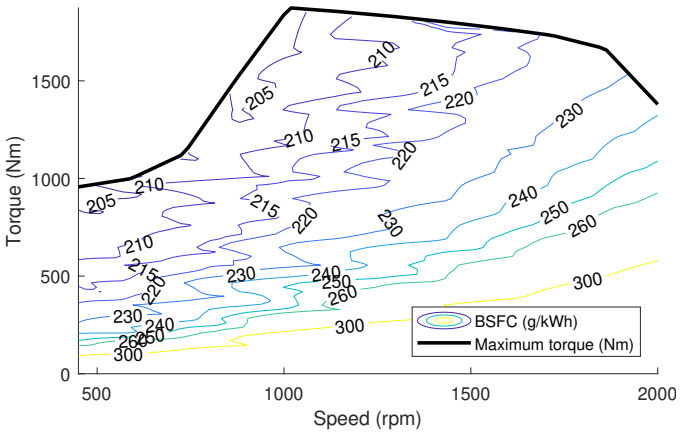

Fig. 1. The torque limit of the engine together with contour lines of the brake-specific fuel consumption (BSFC).

2.4 Transmission system

Vehicle speed and longitudinal force can be calculated from engine speed and torque, respectively, as

$$v(s) = \omega(s)R(\gamma), \quad F_{\mathrm{w}}(s) = \frac{M(s)\eta_\gamma(\gamma)}{R(\gamma)} \tag{8}$$

where γ is selected gear, η_γ is gear efficiency and $R(\gamma)$ is calculated as

$$R(\gamma) = \frac{R_w}{r_\gamma(\gamma) r_{\mathrm{fg}}} \tag{9}$$

where R_w, r_γ and r_{fg} are wheel radius, transmission gear ratio and final drive ratio, respectively.

It follows from (5) and (8) that the maximum longitudinal force the engine can deliver, $F_{\max}(E,\gamma)$, can be expressed as a function of kinetic energy and transmission gear, which will be illustrated later.

3. CONTROL PROBLEM FORMULATION

The problem is formulated to minimize aggregated fuel consumption, by integrating the fuel mass rate $\mu(M,\omega)$. As integration is performed in distance, a division with speed takes place

$$\int_0^{s_f} \frac{\mu(M,\omega)}{v(s)} \mathrm{d}s \tag{10}$$

where s_f is the final position at the end of the route. By replacing the engine speed and torque with the vehicle kinetic energy and longitudinal force according to (5) and (8), it is possible to derive a three-dimensional map $\mu_{\mathrm{w}}(F_{\mathrm{w}},E,\gamma)$. Then, the addressed problem can be formulated as

$$\min_{F_{\mathrm{w}},F_{\mathrm{brk}},\gamma} \int_0^{s_{\mathrm{f}}} \mu_{\mathrm{w}}(F_{\mathrm{w}},E,\gamma)\sqrt{\frac{m}{2E(s)}}\mathrm{d}s \tag{11a}$$

subject to

$$t'(s) = \sqrt{\frac{m}{2E(s)}} \tag{11b}$$

$$E'(s) = F_{\mathrm{w}}(s) + F_{\mathrm{brk}}(s) - \tilde{c}_{\mathrm{a}}E(s) - F_\alpha(s) \tag{11c}$$

$$E(s) \in \frac{m}{2}[v^2_{\min}(s), v^2_{\max}(s)] \tag{11d}$$

$$F_{\mathrm{brk}}(s) \le 0 \tag{11e}$$

$$F_{\mathrm{w}}(s) \in [0, F_{\max}(E,\gamma)] \tag{11f}$$

$$\gamma(s) \in \{1,2,...,\gamma_{\max}\} \tag{11g}$$

$$t(0) = t_0, \quad E(0) = \frac{mv_0^2}{2} \tag{11h}$$

$$t(s_{\mathrm{f}}) \le t_{\mathrm{f}} \tag{11i}$$

where v_0, v_{min} and v_{max} are initial speed, minimum allowable and maximum allowable speeds respectively. Furthermore, t_0, t_{f} and s_{f} are initial travel time, final travel time and final position respectively. Moreover, $F_{\max}(E,\gamma)$ is maximum longitudinal force at the wheel side of the vehicle for given kinetic energy and selected gear. It should be mentioned that F_{w}, F_{brk} and γ are trajectories in terms of s, however it is not written explicitly for simplicity in the above formulation and in several later formulations. The constraints (11b)-(11f) are enforced for all $s \in [0, s_{\mathrm{f}}]$. Problem (11) is a mixed-integer, non-convex and dynamic nonlinear program. It has two states, t and E, two real-valued control variables, F_{w} and F_{brk}, and one integer control variable, γ.

3.1 Driving cycle and velocity constraints

In the studied scenario, a vehicle is traveling over a long horizon in a possibly hilly terrain from Södertälje to Norrköping in Sweden. The driving cycle is the same as it is considered by Eriksson et al. (2016), but with different sampling interval. The reference speed trajectory is constructed based on the preferred cruising speed set by the driver, or set automatically by a telemetry system, using speed filter, see (Murgovski et al., 2016). However, the reference is not necessarily tracked by the vehicle, but can vary within the range of $[v_{\min}(s), v_{\max}(s)]$. According to the obtained reference speed trajectory, the final travel time is the time to reach final position where the vehicle is driven by reference speed, v_r within the receding horizon as

$$t(s_{\mathrm{f}}) \le t_{\mathrm{f}} = \int_0^{s_f} \frac{ds}{v_r(s)}. \tag{12}$$

4. COMPUTATIONALLY EFFICIENT ALGORITHM

This section provides several steps that reformulate problem (11) into a problem that can be solved more efficiently. These steps include 1) a non-approximate bi-level formulation that enables decoupling the gear selection from the dynamic optimization problem; 2) insights from necessary PMP conditions; and 3) approximations that allow the resulting smooth, nonlinear dynamic problem to be solved by SQP, in RTI framework.

4.1 Decoupling of integer variables

It is possible to rewrite problem (11) as a bi-level program

$$\min_{F_{\mathrm{w}},F_{\mathrm{brk}}} \int_0^{s_{\mathrm{f}}} \mu_{\mathrm{w}}(F_{\mathrm{w}},E,\gamma^*)\sqrt{\frac{m}{2E(s)}}\mathrm{d}s \tag{13a}$$

subject to: (11b)-(11e), (11h), (11i),

$$F_{\mathrm{w}}(s) \in [0, F_{\max}(E,\gamma^*)] \tag{13b}$$

$$\gamma^*(s) = \mathrm{argmin}_\gamma\, \mu(F_{\mathrm{w}},E,\gamma) \tag{13c}$$

subject to: $\gamma(s) \in \{1,2,...,\gamma_{\max}\}$ (13d)

$$F_{\mathrm{w}}(s) \in [0, F_{\max}(E,\gamma)] \tag{13e}$$

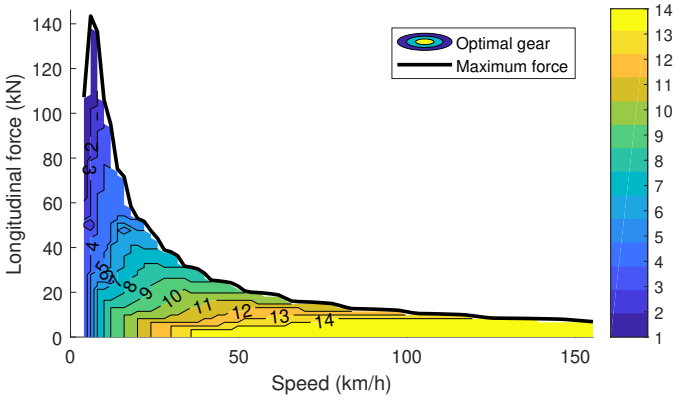

Fig. 2. Optimal gear selection for all feasible operating points in longitudinal force and vehicle speed.

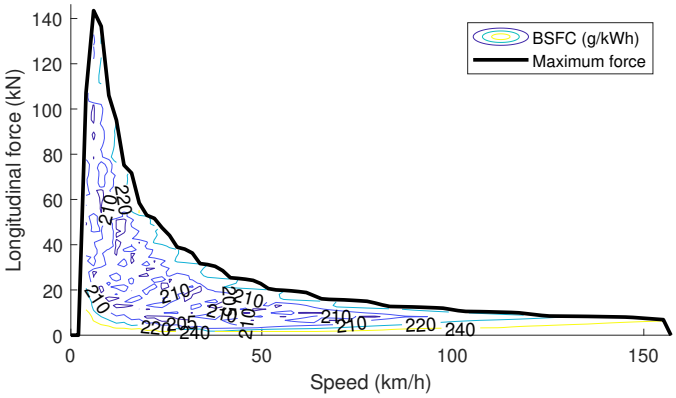

Fig. 3. Optimal brake specific fuel consumption (BSFC) and the maximum longitudinal force that can be delivered by the engine.

where gear optimization has been moved to the lower-level task. It can be observed in (13) that all the system dynamics (states) belong to the higher level task, while the lower-level task is simply a static problem.

It should be reemphasized that since ICE and transmission system are both modeled statically, it is valid to solve the gear selection problem independently from the upper-level task in the lower-level task in (13), by optimizing gear for any feasible combination of values of F_{w} and E. Then, the gear selection problem can be approached by gridding the feasible sets for F_{w} and E and solving

$$f^*_\gamma(F_{\mathrm{w}}, E) = \operatorname{argmin}_\gamma \mu_{\mathrm{w}}(F_{\mathrm{w}}, E, \gamma) \tag{14a}$$
$$\text{subject to: } \gamma \in \{1, 2, ..., \gamma_{\max}\} \tag{14b}$$
$$F_{\mathrm{w}} \in \mathcal{F} \subseteq [0, F_{\max}(E, \gamma)] \tag{14c}$$
$$E \in \mathcal{E} \subseteq m[\omega^2_{\mathrm{idle}}, \omega^2_{\max}]R^2(\gamma)/2 \tag{14d}$$

where the sets $\mathcal{F}, \mathcal{E}$ are discrete, ω_{idle} is the engine idling speed and $\omega_{\max}$ is the maximum speed, above which the engine torque drops to zero. Here, $f^*_\gamma(F_{\mathrm{w}}, E)$ is a two-dimensional map, illustrated in Fig. 2, which holds the optimal gear choices for all force-speed combinations. As a consequence, the three-dimensional fuel map $\mu_{\mathrm{w}}(F_{\mathrm{w}}, E, \gamma)$ and the two dimensional force limit $F_{\max}(E, \gamma)$ can be replaced by a two-dimensional and a one dimensional map, respectively,

$$\mu^*_\gamma(F_{\mathrm{w}}, E) = \mu_{\mathrm{w}}(F_{\mathrm{w}}, E, f^*_\gamma(F_{\mathrm{w}}, E)) \tag{15}$$
$$F_{\gamma\max}(E) = \max_\gamma F_{\max}(E, \gamma). \tag{16}$$

The optimal fuel map including its force limit is illustrated in Fig. 3.

4.2 Necessary conditions for optimality

Here, the idea is to adjoin dynamics of the travel time to the objective. Therefore, the non-convex constraint regarding to the travel time constraint is omitted and its influence on the optimization problem is considered in the objective function. After the optimal gear map is decided, the properties of the resulting dynamic optimization problem (13) can be investigated from the necessary condition for optimality in PMP

$$\lambda'^*_t(s) = -\left(\frac{\partial \mathcal{H}(\cdot)}{\partial t}\right)^* = 0, \quad \lambda'^*_E(s) = -\left(\frac{\partial \mathcal{H}(\cdot)}{\partial E}\right)^* \tag{17}$$

where the Hamiltonian is defined as

$$\mathcal{H}(\cdot) = \mu^*_\gamma(F_{\mathrm{w}}, E)\sqrt{\frac{m}{2E(s)}} + \lambda_t(s)\sqrt{\frac{m}{2E(s)}} + \lambda_E(s)(F_{\mathrm{w}}(s) + F_{\mathrm{brk}}(s) - \tilde{c}_{\mathrm{a}}E(s) - F_\alpha(s)). \tag{18}$$

It can be concluded from (17) that λ^*_t has to be a constant, since the Hamiltonian is not an explicit function of travel time and the time is a strictly monotonically increasing function that may activate constraint (11i) only at the final instant. This property can be exploited to formulate the following dynamic optimization problem

$$\min_{F_{\mathrm{w}}, F_{\mathrm{brk}}} \int_0^{s_{\mathrm{f}}} \left(\mu^*_\gamma(F_{\mathrm{w}}, E)\sqrt{\frac{m}{2E(s)}} + \lambda^*_t\sqrt{\frac{m}{2E(s)}}\right) \mathrm{d}s$$
$$\text{subject to}$$
$$E'(s) = F_{\mathrm{w}}(s) + F_{\mathrm{brk}}(s) - c_{\mathrm{a}}E(s) - F_\alpha(s) \tag{19a}$$
$$E(s) \in \frac{m}{2}[v^2_{\min}(s), v^2_{\max}(s)] \tag{19b}$$
$$F_{\mathrm{brk}}(s) \le 0 \tag{19c}$$
$$F_{\mathrm{w}}(s) \in [0, F_{\gamma\max}(E)] \tag{19d}$$
$$E(0) = \frac{mv_0^2}{2} \tag{19e}$$

where the travel time dynamics have been adjoined to the objective, given the optimal costate λ^*_t that satisfies the final time constraint (11i). For more information about PMP theory and its applications in automotive industry, see, e.g. (Pontryagin et al., 1962), (Murgovski et al., 2013b), and references therein.

In turn, the optimal costate λ^*_t can be obtained as a solution of a two-point boundary value problem (2PBVP), where the optimal solution is expected to result in a travel time that is as close as possible to t_f, since arriving sooner at the destination requires more fuel, in general. The solution of the 2PBVP can be obtained by repeatedly solving problem (19) using the following algorithm:

(1) Solve problem (19) for a given $\lambda_t^{(k)}$ and simulate forward the time dynamics with the optimal control, in order to obtain the difference $\Delta t_{\mathrm{f}}^{(k)} = t_{\mathrm{f}} - t(s_{\mathrm{f}})$.
(2) If $\Delta t_{\mathrm{f}}^{(k)} \le$ threshold, terminate the loop.
(3) Update $\lambda_t^{(k+1)} = \lambda_t^{(k)} + \delta\,\mathrm{sign}(\Delta t_{\mathrm{f}}^{(k)})$.
(4) If $\mathrm{sign}(\Delta t_{\mathrm{f}}^{(k)}) \neq \mathrm{sign}(\Delta t_{\mathrm{f}}^{(k-1)})$, then $\delta \leftarrow \delta/2$.
(5) Start new iteration, i.e. $k \leftarrow k+1$ and go to (1).

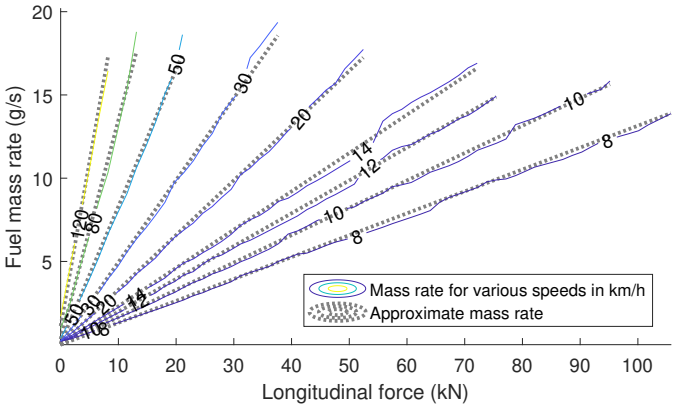

Fig. 4. Original and approximate fuel mass rate for various vehicle velocities and longitudinal forces.

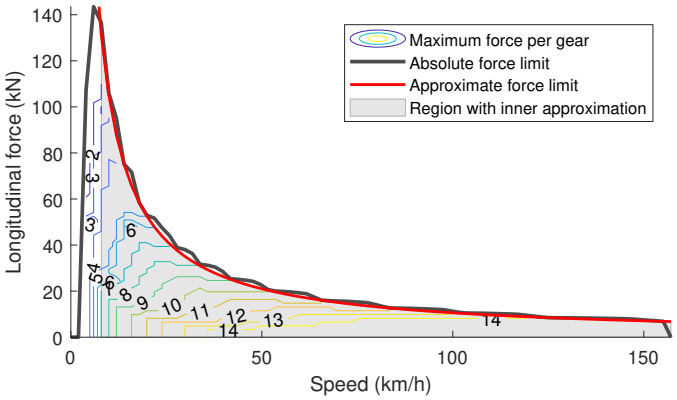

Fig. 5. Approximate and the original force limit. The approximate limit is an inner approximation in the shaded region, i.e. for speed above 8 km/h.

Problem (19) is a dynamic nonlinear program that can be solved in several ways. Due to having only a single state, the kinetic energy, problem (19) can be solved with Dynamic Programming (DP), which could be computational efficient for short look-ahead horizons. As the goal of this paper is to optimize over a long look-ahead horizon, possibly to the end of the route, approximation steps are investigated to further decrease the computational effort.

4.3 Sequential quadratic programming

Once the constraint on travel time is adjoined to the objective, the resulting optimization problem can be solved directly. The basic idea of direct methods (DM) is to derive direct transcription of optimal control problem, which is basically the approximations of state and actuator trajectories to different forms of functions. Therefore, the original optimal control problem is transformed to a discrete optimization problem. To gain more insight of DM in automotive applications, see e.g., (Asprion et al., 2014) and (Macian et al., 2018). Problem (19) includes two look-up tables, $\mu^*_\gamma(F_\mathrm{w}, E)$ and $F_{\gamma\max}(E)$, which are fitted here with analytic expressions. The fuel consumption is approximated by the following function

$$\tilde{\mu}^*_\gamma(F_\mathrm{w}, v) = a_0 + a_1 v^3(s) + a_2 v(s) F_\mathrm{w}(s) \qquad (20)$$

with $a_0, a_1, a_2 \geq 0$. Similar functions have been investigated by Murgovski et al. (2016); Hovgard et al. (2018), where higher order terms in speed and force (or torque) have been included. Fig. 4 shows that for the studied engine model it is sufficient to use a first order term in F_w, although it is possible, without significant increase in computational effort, to include higher order terms as well.

Then, considering kinetic energy instead of velocity the term in the objective,

$$\tilde{\mu}^*_\gamma(F_\mathrm{w}, E)\sqrt{\frac{m}{2E(s)}} = \frac{a_0\sqrt{m}}{\sqrt{2E(s)}} + \frac{2a_1}{m}E(s) + a_2 F_\mathrm{w}(s)$$

becomes a convex second order cone function in E and F_w. Accordingly, the stage cost in problem (19),

$$V(E, F_\mathrm{w}) = \frac{(a_0 + \lambda^*_t)\sqrt{m}}{\sqrt{2E(s)}} + \frac{2a_1}{m}E(s) + a_2 F_\mathrm{w}(s) \qquad (21)$$

is also a convex second order cone function.

The force limit $F_{\gamma\max}(E)$ is approximated by

$$\tilde{F}_{\gamma\max}(E) = b_0 + \frac{b_1\sqrt{m}}{\sqrt{E(s)}} \qquad (22)$$

where b_1 resembles the maximum engine power, as it can be alternatively written as a division of power with vehicle speed. The approximated force limit is an inner approximation of the original force for speeds above 8 km/h, see Fig. 5, which is acceptable for the highway scenarios investigated in this paper. The obtained inner approximation is the solution of a linear program. (See Appendix A for details.)

The resulting optimization problem is not convex, due to the nonlinear term $f(E) = 1/\sqrt{E(s)}$ in (22), which due to the sign of b_1 is a convex function (a convex problem, though, requires a concave function here). Therefore, linearizing it about a trajectory $\hat{E}(s)$,

$$f_\mathrm{lin}(E, \hat{E}) = f(\hat{E}) + \left.\frac{\mathrm{d}f(E)}{\mathrm{d}E}\right|_{\hat{E}} (E(s) - \hat{E}(s)) \qquad (23)$$

provides a convex inner approximation. This allows developing a computationally efficient SQP based on RTI (Diehl, 2001).

RTI exploits the iterative nature of MPC, by spreading the sequential programming iterations over the MPC updates. The idea is to solve only one convex program in each MPC update, which significantly reduces computational effort and allows the usage of standard convex solvers. The trade-off is the early termination of the sequential algorithm, which may not converge to an optimum, especially in the initial MPC stages. However, as it has been shown that the approximation (23) is conservative, see 5, it can be guaranteed that despite possibly being suboptimal, all obtained solutions (if such solutions exist) are also feasible in the original non-approximate problem.

The resulting optimization problem is a convex second order cone program (SOCP), which can be solved efficiently with off the shelf solvers. However, to further reduce computational effort, we propose to approximate the stage cost as a quadratic function, since QP technology is more mature than SOCP, and can, in general, be solved more efficiently. Thus, a second order approximation is performed about $\hat{E}$,

$$f_{\text{quad}}(E,\hat{E}) = f_{\text{lin}}(E,\hat{E}) + \frac{1}{2}\frac{\mathrm{d}^2 f(E)}{\mathrm{d}E^2}\bigg|_{\hat{E}} (E(s)-\hat{E}(s))^2$$

and the stage cost is approximated by

$$\tilde{V}(\cdot) = f_{\text{quad}}(E,\hat{E})\frac{(a_0+\lambda_t^*)\sqrt{m}}{\sqrt{2}} + \frac{2a_1}{m}E(s) + a_2 F_{\text{w}}(s).$$

Finally, the dynamic optimization problem can be summarized as the QP,

$$\min_{F_{\text{w}},F_{\text{brk}}} \int_0^{s_{\text{f}}} \Big(\tilde{V}(E,F_{\text{w}},\hat{E}) + Q(\cdot)\Big)\,\mathrm{d}s$$

subject to

$$E'(s) = F_{\text{w}}(s) + F_{\text{brk}}(s) - c_{\text{a}}E(s) - F_{\alpha}(s) \tag{24a}$$

$$E(s) \in \frac{m}{2}[v_{\min}^2(s), v_{\max}^2(s)] \tag{24b}$$

$$F_{\text{brk}}(s) \leq 0 \tag{24c}$$

$$F_{\text{w}}(s) \in [0, b_0 + b_1\sqrt{m} f_{\text{lin}}(E,\hat{E})] \tag{24d}$$

$$E(0) = \frac{m v_0^2}{2} \tag{24e}$$

where the term Q in the objective is a standard term in the SQP framework that provides additional search direction towards the optimal solution that also minimizes the linearization error. It includes Hessian of the Lagrangian and Jacobian of the objective function, with respect to the optimization variables. For further details, see Nocedal and Wright (2006). It has been found in this paper that the linearized constraint on the force limit gets rarely activated and the term Q has little influence on the convergence. Therefore, it has been assumed to be zero.

After each QP iteration, the trajectory about which the problem is linearized is updated by moving towards the direction of the current optimal solution, i.e.

$$\hat{E}^{(k+1)}(s) = \hat{E}^{(k)}(s) + \beta(E^{*(k)}(s) - \hat{E}^{(k)}(s)) \tag{25}$$

where β is the step size that regulates the convergence rate.

5. RESULTS

In this section, optimal velocity profile as well as longitudinal force and braking force of the vehicle in the wheel side are shown. In addition, convergence of the proposed algorithm to the optimal solution is demonstrated. Finally, the computation time for different sampling intervals of the entire horizon is calculated. These investigations are done for single conventional vehicle scenario driving in the driving cycle from Södertälje to Norrköping.

5.1 Optimal velocity

As shown in Fig. 6a, velocity profile of the vehicle is optimized, where the vehicle is driving in a hilly topography. Considering Fig. 6b, it can be observed that the proposed algorithm properly reduces braking by fully utilizing the accumulation of kinetic energy. In other words, it can be noticed that before reaching a steep downhill, the algorithm decelerates the vehicle until the minimum allowed speed is reached, thus emptying the kinetic energy buffer. During the following downhill segment, the vehicle builds up kinetic energy, until the upper speed limit is reached. As there is no additional room for storing kinetic energy

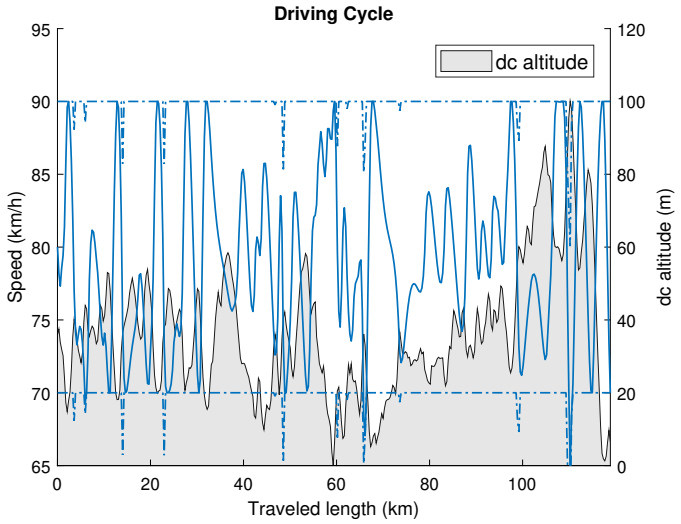

(a)

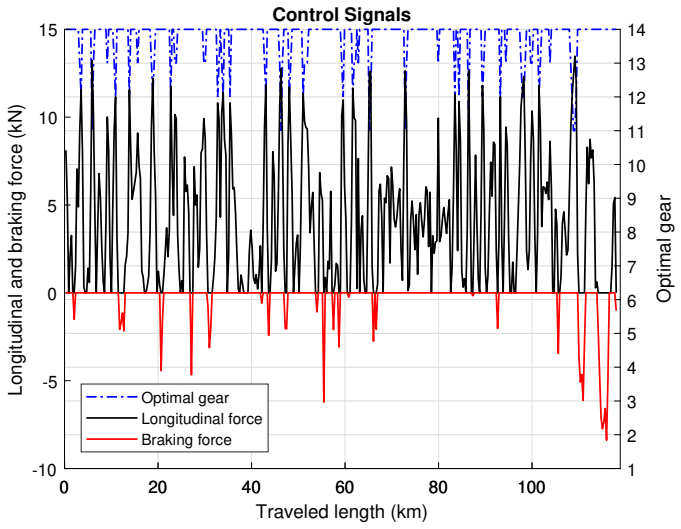

(b)

Fig. 6. (a) Optimal velocity profile together with road topography, (b) longitudinal force and braking force.

after maximum speed is reached, the vehicle will eventually need to apply the brakes. Although being fuel optimal, the resulting velocity trajectory may not be a comfortable one. This indicates that in order to have smoother velocity profile, discomfort penalties also need to be included as a part of the cost function, e.g. penalties on longitudinal acceleration and jerk. Alternatively, you may directly write the space derivatives. This is possible, since the problem is still kept in continuous space, e.g.

$$\min_{F_{\text{w}},F_{\text{brk}}} \int_0^{s_{\text{f}}} \Big(\tilde{V}(E,F_{\text{w}},\hat{E}) + w_1 E'^2(s) + w_2 E''^2(s)\Big)\,\mathrm{d}s$$

where, w_1 and w_2 are weighting parameters. Here, the preferred cruising speed is set to $80 km/h$, where the optimal velocity is allowed to vary between upper and lower bounds. The maximum allowed travel time has been computed as 5371 seconds. Furthermore, calculated costate of time is $0.0048 kg/s$. Weighting parameters, w_1 and w_2, are assumed to be 100 and 1000 respectively.

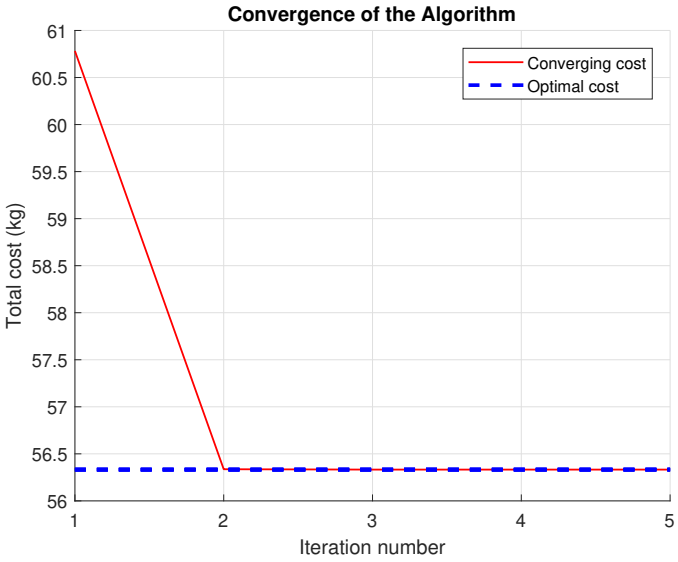

Fig. 7. Convergence of the algorithm; in the first two iterations total cost converges rapidly to the optimum.

5.2 Algorithm convergence

As it is mentioned earlier for the studied driving cycle the gear trajectory is optimized offline in the lower level of the optimization problem. Consequently the SQP (24) converges to local optimum in 5 iterations, see Fig. 7. The local optimum value is obtained by solving the SOCP (19), where there is no approximation in the objective function. It should be noticed that the initial value of the objective function is calculated based on the obtained kinetic energy and longitudinal force from the speed prefilter. Rest of objective function values are obtained by solving the SQP. Here, the sampling interval and convergence step are assumed as $N = 400$ and $\beta = 0.96$ respectively. Relative linearization error is less than 0.01%. For future studies, it is possible to solve one QP in each MPC update rather than waiting for the convergence by solving SQP, since the value of the objective function in the second iteration (the solution of SQP in the first iteration) is very close to the local optimum and it is highly possible to reach the local optimum in the long horizon by solving the MPC algorithm.

5.3 Computation time

For the considered driving cycle with various sampling intervals, the computation time of ECOS for solving problem (24) is demonstrated in Fig. 8. It should be mentioned that the iterations for finding the costate of time is not included here and Fig. 8 shows the needed time for solving a single QP for a given costate of time value, because the idea is to search for the optimal costate across MPC updates. After moving the horizon the next MPC is solved, then the costate of time is updated based on the algorithm given in 4.2. The PC properties are: 6600K CPU at 2.81GHz and 16GB RAM. It can be observed that for higher sampling intervals, the computational time increases. Thus, for real-time applications, it is preferable to have small sampling interval, however the information on the topography should not be lost.

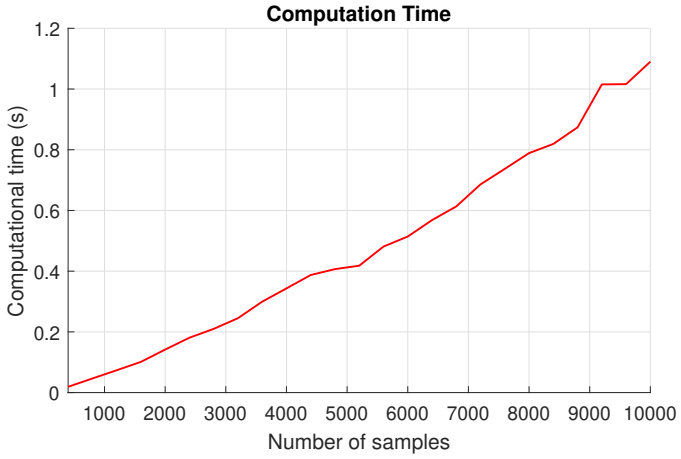

Fig. 8. Computation time of the algorithm increases with the number of samples.

6. CONCLUSION

In this paper, a fast predictive control approach for a heavy-duty vehicle driving in a possibly hilly terrain is presented, where the traveling horizon can be stretched to hundreds of kilometers. The control architecture includes two levels, which decouple gear selection from real-valued decisions. Optimal gear selection and fuel consumption maps for feasible longitudinal force and kinetic energy pairs are computed by offline optimization. The remaining nonlinear dynamic problem is considered as on-line optimization, where the travel time is adjoined to the objective function and sequential quadratic programming is employed to calculate optimal velocity profile of the vehicle. The proposed algorithm shows interesting results in respect of convergence rate and computation time, which are important factors for a computationally efficient approach over a long look-ahead horizon.

Appendix A. APPROXIMATION OF MAXIMUM LONGITUDINAL FORCE

To approximate the maximum force limit for speeds above $8km/h$, (22), as an inner approximation of the original nonlinear and non-smooth limit, a linear program is solved as:

$$\begin{aligned} &\min_{x} \left(f^T x\right) \\ &\text{subject to} \\ &Ax \leq b \end{aligned}$$

where

$$f = -\begin{bmatrix} v_{\max} - v_1 \\ \ln(v_{\max}) - \ln(v_1) \end{bmatrix}, x = \begin{bmatrix} x1 \\ x2 \end{bmatrix}$$

and

$$A = \begin{bmatrix} 1 & \frac{1}{v} \end{bmatrix}, b = F_{\max}(v)$$

where the vehicle speed, v is allowed to vary between two limits

$$v \in [v_1, v_{\max}]$$

where $v_1 = 8km/h$ and $v_{\max}$ is the maximum reachable speed by the vehicle. In this formulation, the idea is to minimize the area between the original force limit and the inner approximation.

REFERENCES

J. Asprion, O. Chinellato, and L. Guzzella. Optimal control of diesel engines: numerical methods, applications, and experimental validation. *Math Probl Eng*, pages 1–21, 2014.

J. N. Barkenbus. Eco-driving: An overlooked climate change initiative. *Energy Policy*, 38(2):762–769, 2010.

R. Bellman. *Dynamic Programming*. Princeton Univ Pr, New Jersey, 1957.

R. de Castro, M. Tanelli, R. E. Araújo, and S. M. Savaresi. Minimum-time path-following for highly redundant electric vehicles. *IEEE Transactions on Control Systems Technology*, 24(2):487–501, 2016.

M. Diehl. *Real-Time Optimization for Large Scale Nonlinear Processes*. PhD thesis, University of Heidelberg, 2001.

L. Eriksson, A. Larsson, and A. Thomasson. Heavy duty truck on open road - the aac 2016 benchmark. In *8th IFAC Symposium on Advances in Automotive Control*, Kolmården, Sweden, 2016.

E. Hellström, M. Ivarsson, J. Åslund, and L. Nielsen. Look-ahead control for heavy trucks to minimize trip time and fuel consumption. *Control Engineering Practice*, 17(2):245–254, 2009.

E. Hellström, J. Åslund, and L. Nielsen. Design of an efficient algorithm for fuel-optimal look-ahead control. *Control Engineering Practice*, 18(11):1318–1327, 2010.

E. Hellström, J. Åslund, and L. Nielsen. Management of kinetic and electric energy in heavy trucks. *SAE International Journal of Engines*, 3(1):1152–1163, 2010.

G. Heppeler, M. Sonntag, U. Wohlhaupter, and O. Sawodny. Predictive planning of optimal velocity and state of charge trajectories for hybrid electric vehicles. *Control Engineering Practice*, 61:229–243, 2016.

M. Hovgard, O. Jonsson, N. Murgovski, M. Sanfridson, and J. Fredriksson. Cooperative energy management of electrified vehicles on hilly roads. *Control Engineering Practice*, 73:66–78, 2018.

L. Johannesson, N. Murgovski, E. Jonasson, J. Hellgren, and B. Egardt. Predictive energy management of hybrid long-haul trucks. *Control Engineering Practice*, 41:83–97, 2015a.

L. Johannesson, M. Nilsson, and N. Murgovski. Look-ahead vehicle energy management with traffic predictions. In *IFAC Workshop on Engine and Powertrain Control, Simulation and Modeling (E-COSM)*, volume 48, pages 244–251, Columbus, Ohio, USA, 2015b.

O. Lindgärde, L. Feng, A. Tenstam, and M. Soderman. Optimal vehicle control for fuel efficiency. *SAE International Journal of Commercial Vehicles*, 8(2):682–694, 2015.

T. Lipp and S. Boyd. Minimum-time speed optimization along a fixed path. *International Journal of Control*, 87 (6):1297–1311, 2014.

V. Macian, C. Guardiola, B. Pla, and A. Reig. Application and benchmarking of a direct method to optimize the fuel consumption of a diesel electric locomotive. *Proc IMechE Part F: J Rail and Rapid Transit*, 2018. doi: 10.1177/0954409718772133.

D. Mayne, J. Rawlings, C. Rao, and P. Scokaert. Constrained model predictive control : Stability and optimality. *Automatica*, 36(6):789–814, 2000.

N. Murgovski, L. Johannesson, J. Sjöberg, and B. Egardt. Component sizing of a plug-in hybrid electric powertrain via convex optimization. *Mechatronics*, 22(1):106–120, 2012.

N. Murgovski, X. Hu, L. Johannesson, and B. Egardt. Filtering driving cycles for assessment of electrified vehicles. In *Workshop for new energy vehicle dynamic system and control technology*, Beijing, China, 2013a.

N. Murgovski, L. Johannesson, and J. Sjöberg. Engine on/off control for dimensioning hybrid electric powertrains via convex optimization. *IEEE Transactions on Vehicular Technology*, 62(7):2949–2962, 2013b.

N. Murgovski, L. Johannesson, X. Hu, B. Egardt, and J. Sjöberg. Convex relaxations in the optimal control of electrified vehicles. In *American Control Conference*, Chicago, USA, 2015.

N. Murgovski, B. Egardt, and M. Nilsson. Cooperative energy management of automated vehicles. *Control Engineering Practice*, 57:84–98, 2016.

V. Ngo, T. Hofman, M. Steinbuch, and A. Serrarens. Optimal control of the gearshift command for hybrid electric vehicles. *IEEE Transactions On Vehicular Technology*, 61(8):3531–3543, 2012.

J. Nocedal and S. J. Wright. *Numerical Optimization*. Springer, 2006.

L. S. Pontryagin, V. G. Boltyanskii, R. V. Gamkrelidze, and E. F. Mishchenko. *The Mathematical Theory of Optimal Processes*. Interscience Publishers, 1962.

M. Pourabdollah, N. Murgovski, A. Grauers, and B. Egardt. Optimal sizing of a parallel PHEV powertrain. *IEEE Transactions on Vehicular Technology*, 62 (6):2469–2480, 2013.

S. Uebel, N. Murgovski, C. Tempelhahn, and B. Bäker. Optimal energy management and velocity control of hybrid electric vehicles. *IEEE Transactions on Vehicular Technology*, PP(99):1–1, 2017. doi: 10.1109/TVT.2017.2727680.

T. van Keulen, B. de Jager, D. Foster, and M. Steinbuch. Velocity trajectory optimization in hybrid electric trucks. In *American Control Conference*, pages 5074–5079, Marriott Waterfront, Baltimore, MD, USA, 2010.

T. van Keulen, B. de Jager, and M. Steinbuch. Optimal trajectories for vehicles with energy recovery options. In *IFAC World Congress*, pages 3831–3836, Milan, Italy, 2011.

T. van Keulen, J. Gillot, B. de Jager, and M. Steinbuch. Solution for state constrained optimal control problems applied to power split control for hybrid vehicles. *Automatica*, 50(1):187–192, 2014.

J. Wahlström and L. Eriksson. Modelling diesel engines with a variable-geometry turbocharger and exhaust gas recirculation by optimization of model parameters for capturing non-linear system dynamics. *Sage journals*, 225(7):960–986, 2012.